

MULTI-WAVELENGTH LIGHT-CURVE FITTING OF YOUNG AND MILLISECOND PULSARS

J. P  tri¹

Abstract. Since the launch of the Fermi γ -ray telescope, several hundred radio-loud γ -ray pulsars have been detected, some belonging to the millisecond pulsars and some part of the young pulsar population (with spin periods longer than 30 ms). Observing simultaneously pulsed radio and γ -ray emission from these stars helps to constrain the geometry and radiation mechanisms within their magnetosphere and to localize the photon production sites. In this work we show how time-aligned γ -ray light curve fitting of young and millisecond pulsars constrain their magnetospheric configuration, namely the magnetic axis and line-of-sight inclination angles. To this end, we assume a dipole force-free magnetosphere where radio photons emanate from high altitudes above the polar caps and γ -rays originate from the pulsar striped wind. Further constraints were obtained from radio polarization measurements, if available, following the rotating vector model, including aberration and retardation effects. We are currently extending our analysis to thermal and non-thermal X-ray emission using observations from several X-ray telescopes. Preliminary results applied to a bright pulsar show that the non-thermal X-rays are produced between 20% and 55% of the light cylinder radius.

Keywords: neutron stars, magnetic fields, rotation, pulsars, radio emission, γ -rays, X-rays

1 Introduction

The multi-wavelength pulsed emission of pulsars is very sensitive to their global geometry constrained by the angles between the rotation axis and the magnetic dipole moment and between the rotation axis and the line of sight. Several works in the past showed that a simultaneous radio and γ -ray light-curve fitting is valuable to pin down the geometry. For instance P  tri (2011) showed that in the framework of a force-free split-monopole solution, simple analytical expressions for the radio time lag and the γ -ray peak separation can be derived. Refinements with a dipolar force-free magnetosphere model have been given by Benli et al. (2021) for millisecond pulsars and by P  tri & Mitra (2021) for young pulsars. Other useful constraints on the emission sites come from detailed radio polarization observations if available. However, polarization data from millisecond pulsars are difficult to interpret because of the presence of strong non dipolar fields at the photon production sites. In section 2 the phase-aligned γ -ray light curve fitting is studied whereas in section 3 the thermal and non-thermal X-rays are fitted. Conclusions are drawn in section 4.

2 Gamma-ray light-curve fitting

To fit the γ -ray light-curves of pulsars, we distinguish between millisecond and young pulsars because for the latter, the radio emission altitude corresponds to regions where the magnetic field is essentially dipolar and good radio polarization data are available. Therefore, thanks to the rotating vector model (Radhakrishnan & Cooke 1969), it is possible to infer the radio emission height and to relate the magnetic obliquity to the observer line of sight inclination angle.

¹ Universit   de Strasbourg, CNRS, Observatoire astronomique de Strasbourg, UMR 7550, F-67000 Strasbourg, France.

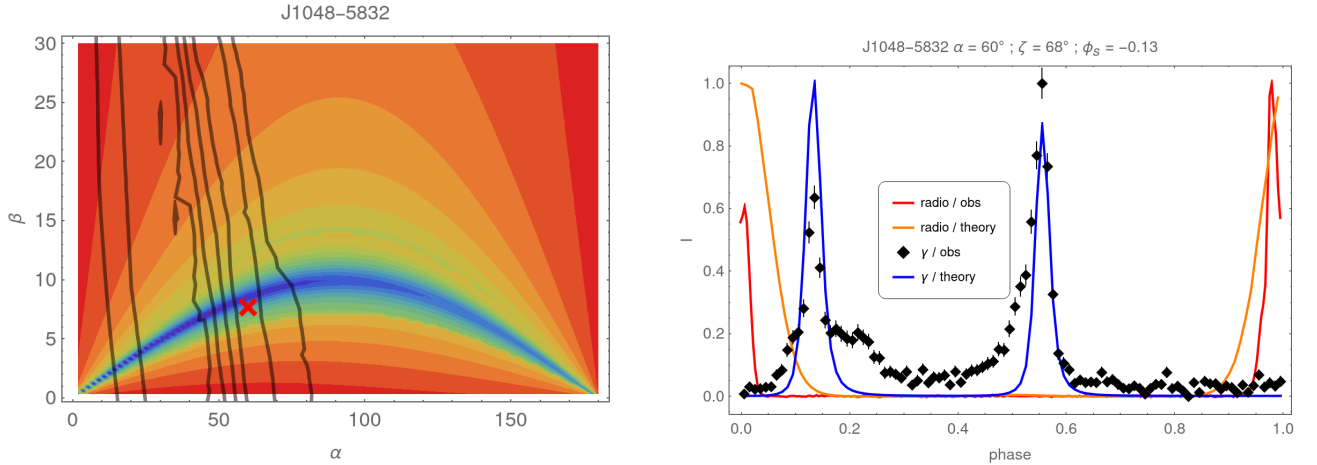


Fig. 1. Best fit for the young pulsar J1048-5832. On the left panel, the $\log \chi^2$ contour plots, in colour contours for radio polarization fits, and in solid coloured lines for γ -ray light-curves. The red cross indicates the best jointed radio/ γ -ray fit. On the right panel, the associated γ -ray light-curve for the geometry given by the red cross.

2.1 Young pulsars

In our first sample of pulsars (Pétri & Mitra 2021), we selected those with periods larger than 30 ms and with good quality γ -ray pulse profiles from the Fermi/LAT second pulsar catalogue (Abdo et al. 2013). These are non-recycled young pulsars some of them with good linear polarization data. Next, we computed a full atlas of radio and γ -ray pulse profiles depending on the magnetic axis obliquity and line of sight inclination with respect to the neutron star rotation axis. By applying a χ^2 fitting technique to the γ -ray data, we were able to pin down accurately the magnetosphere geometry. Further constraints were obtained from radio polarization measurement following the rotating vector model, including aberration and retardation effects.

Fig. 1 shows an example of best fit for PSR J1048-5832. It is a γ -ray pulsar of period 124 ms with very good quality radio polarization data. It shows two narrow and prominent γ -ray pulses. The radio polarisation data give a relation between α and $\beta = \zeta - \alpha$ as shown in the left panel whereas the γ -ray fit is shown on the right panel with $\alpha = 60^\circ$ and $\zeta = 68^\circ$ with an offset of $\phi_s = -0.13$.

2.2 Millisecond pulsars

In our second sample (Benli et al. 2021), we selected millisecond pulsars (MSPs) with good γ -ray pulse profile also from the second pulsar catalogue. Contrary to the young pulsars, the polarization data are not usable to fit to the rotating vector model because for millisecond pulsars, the light-cylinder radius is much smaller and small scale surface multipole components can strongly affect the polarization position angle. Thus for MSPs we can only rely on the time lag between the γ -ray and the radio pulse profile and on the γ -ray pulse separation.

As an example, Fig.2 shows results for PSR J0030+0451, a MSP with $P = 4.87$ ms possessing a double pulse profile in γ -rays. As can be seen on the left panel, the best fit to the γ -ray light curve was obtained by fixing $\alpha = 70^\circ$, $\zeta = 60^\circ$ and an offset $\phi_s = -0.07$. The right panel shows a crescent shape polar cap and an almost circular polar cap as described by Riley et al. (2019).

3 X-ray light-curve fitting

To complete the multi-wavelength study we need to address the thermal and non-thermal X-ray emission. The former is produced by heating the neutron star surface due to particle bombardment from the magnetosphere or internal heat. Pulsed emission is expected when the polar cap are hotter than the rest of the surface. The location and the size of these polar caps depend on the magnetic field structure in the crust. The latter radiation emanates from higher altitudes within the magnetosphere.

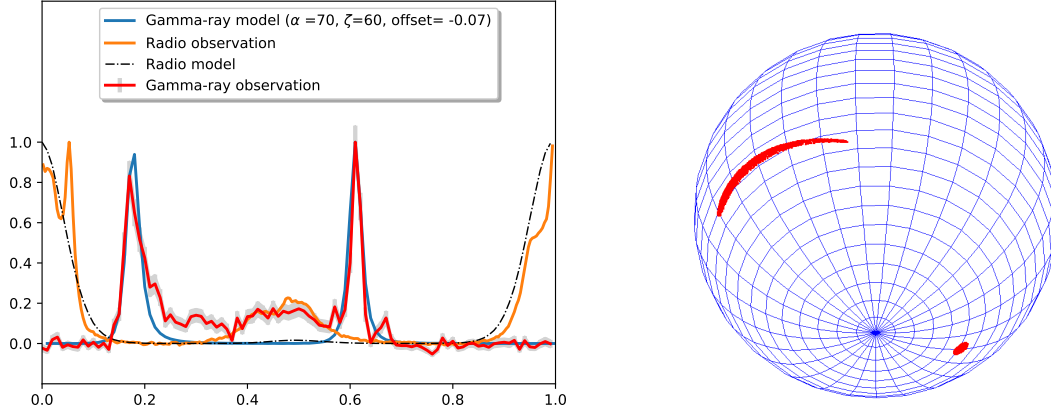


Fig. 2. Best fit for the millisecond pulsar J0030+0451 on the left panel and hot spot geometry from an off-centred dipole plus a small scale surface dipole on the right panel.

3.1 Thermal X-ray

The NICER mission is dedicated to constrain the mass and radius of neutron stars by modelling the pulse profile in the thermal X-ray band. A handful millisecond pulsars have already been investigated by several groups (Riley et al. 2019; Miller et al. 2019). They found the shape, size and location of the hot spots, of which they are usually two. For PSR J0030+0451, they found two hot spots located in the same hemisphere. If the magnetic field is dipolar, this is a strong hint of an off-centred dipole geometry. Moreover the crescent shape of one of this spot suggests the presence of a small scale surface dipole on top of one polar cap, right panel of fig. 2. Base on this idea and on the γ -ray light-curve fits as shown in the previous section, we were able to confirm the line of sight inclination angle of $\zeta \approx 54^\circ$ and the obliquity about $\alpha = 70^\circ$, (Pétri et al. 2023). Therefore phased-aligned γ -ray light-curve studies independently of the thermal X-ray studies agree each other on the same geometry which is thus a robust result. With this first success, we plan to investigate several other NICER pulsars for instance PSR J0740+6620 for which a detailed investigation have already been published by Riley et al. (2021) and Miller et al. (2021).

3.2 Non thermal X-ray

Contrary to the previous energy bands, radio, γ and thermal X-ray, the non-thermal X-ray emission sites and mechanisms are still largely unconstrained. In a last investigation, based again on the γ -ray phased aligned light-curve modelling, we selected young and radio-loud γ -ray pulsars that are also bright in non-thermal X-rays, above 1-2 keV. PSR J2229+6114 is a particularly good candidate. Its geometry is known from Pétri & Mitra (2021) and has been re-explored recently using the third pulsar catalogue 3PC (Smith et al. 2023). Our best fit is shown on the left panel of Fig. 3. Only the X-ray emission altitude and extension need to be fixed. To this end, we computed a comprehensive atlas of X-ray pulse profiles based on the slot gap model, assuming emission only along the separatrix within the light-cylinder. X-ray data are available from NICER (1–10 keV), RXTE (9.4–22.4 keV) and NuSTAR (3–10 keV). The X-ray pulse profiles are compatible with curvature radiation of the primary beam from an emission height in $r/r_L \in [0.2, 0.55]$ and an obliquity $\alpha \in [45^\circ, 50^\circ]$. Moreover the line of sight inclination agrees with γ -ray fit $\zeta \in [34^\circ, 48^\circ]$. The right panel of fig. 3 shows the fit obtained with RXTE.

4 Conclusions

We find good agreement between our emission model and the time-aligned single- or double-peaked γ -ray pulsar observations. We deduce the magnetic inclination angle and the observer line-of-sight with respect to the rotation axis within a small error bar. The distinction between radio-loud or radio-quiet γ -ray pulsars or only radio pulsars is entirely related to the geometry of the associated emitting regions.

The high-altitude polar cap model combined with the striped wind represents a minimalistic approach able to reproduce a wealth of γ -ray pulse profiles for the whole population of pulsars. Based on self-consistent

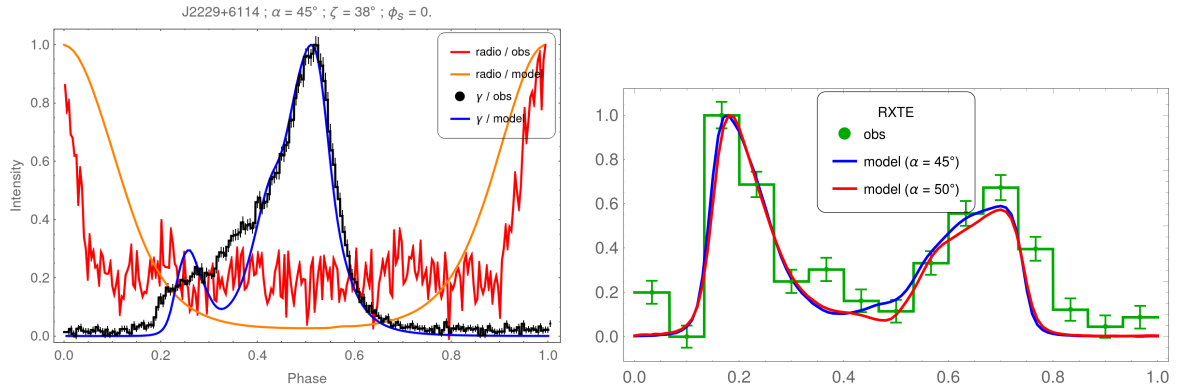


Fig. 3. Best fit of PSR J2229+6114 using the 3PC for γ -rays on the left panel and using the RXTE data in the range 9.4–22.4 keV on the right panel.

force-free simulations, it gives a full geometrical picture of the emission properties without resorting to detailed knowledge of the individual particle dynamics and energetics. For the first time it becomes possible to localize with high confidence the non-thermal X-ray emission sites within the magnetosphere.

This work has been supported by the CEFIPRA grant IFC/F5904-B/2018 and ANR-20-CE31-0010.

References

- Abdo, A. A., Ajello, M., Allafort, A., et al. 2013, *ApJS*, 208, 17
 Benli, O., Pétri, J., & Mitra, D. 2021, *A&A*, 647, A101
 Miller, M. C., Lamb, F. K., Dittmann, A. J., et al. 2019, *ApJL*, 887, L24
 Miller, M. C., Lamb, F. K., Dittmann, A. J., et al. 2021, *ApJ*, 918, L28
 Pétri, J. 2011, *MNRAS*, 412, 1870
 Pétri, J., Guillot, S., Guillemot, L., et al. 2023, arXiv:2309.03620
 Pétri, J. & Mitra, D. 2021, *A&A*, 654, A106
 Radhakrishnan, V. & Cooke, D. J. 1969, *Ap. Lett.*, 3, 225
 Riley, T. E., Watts, A. L., Bogdanov, S., et al. 2019, *ApJL*, 887, L21
 Riley, T. E., Watts, A. L., Ray, P. S., et al. 2021, *ApJ*, 918, L27
 Smith, D. A., Bruel, P., Clark, C. J., et al. 2023, arXiv:2307.11132